JOURNAL OF SOLID STATE CHEMISTRY 118, 341–356 (1995)

Infrared and Polarized Raman Spectra of $M_6[TeMo_6O_{24}] \cdot 7H_2O$[$M$ = K, NH_4] and $(NH_4)_6[TeMo_6O_{24}] \cdot Te(OH)_6 \cdot 7H_2O$ Single Crystals

R. Ratheesh, G. Suresh, and V. U. Nayar[1]

Department of Physics, University of Kerala, Kariavattom, Trivandrum 695 581, India

Received November 14, 1994; accepted March 3, 1995

Heteropolymolybdates are widely used as industrial catalysts, ion exchange agents, corrosion inhibitors, and solid state electrolytes for fuel cells. The infrared (IR) and polarized Raman spectra of $K_6[TeMo_6O_{24}] \cdot 7H_2O$, $(NH_4)_6[TeMo_6O_{24}] \cdot 7H_2O$, and $(NH_4)_6[TeMo_6O_{24}] \cdot Te(OH)_6 \cdot 7H_2O$ single crystals have been recorded and analyzed. The Te–O vibrations and the bridging and terminal Mo–O vibrations observed in the IR and Raman spectra confirm a finite $[TeMo_6O_{24}]^{6-}$ heteropolyanion in all the three crystals. TeO_6 octahedra are considerably distorted in NTMH1 and NTMH2 crystals, while the distortion is less in KTMH. The NH_4^+ ion does not rotate freely in the crystalline lattice and the N–H···O bonds form an asymmetric potential in both ammonium-containing crystals. Stretching and bending vibrations of water molecules show hydrogen bonds of various strengths in all three crystals. Two crystallographically distinct water molecules are identified in KTMH crystal. © 1995 Academic Press, Inc.

INTRODUCTION

Heteropolymolybdates are widely used as industrial catalysts, ion exchange agents, corrosion inhibitors, and solid state electrolytes for fuel cells (1, 2). Studies by Keggin in heteropolyacids, metatungstates, and metamolybdates have confirmed that the polyacid anion can be regarded as a coordination structure, built up of polyhedra of oxygen ions (3). X-ray crystallographic studies of $K_6[TeMo_6O_{24}] \cdot 7H_2O$, $(NH_4)_6[TeMo_6O_{24}] \cdot 7H_2O$, and $(NH_4)_6[TeMo_6O_{24}] \cdot Te(OH)_6 \cdot 7H_2O$ have been known for a long time (4–6). According to Evans these salts contain the heteropolyanion $[TeMo_6O_{24}]^{6-}$, which consists of a TeO_6 octahedron surrounded by six MoO_6 octahedra. Vibrational analysis of a series of polycrystalline telluromolybdate salts has been reported by Grabowski *et al.* (7). In the present investigation, IR and polarized Raman spectra of $K_6[TeMo_6O_{24}] \cdot 7H_2O$, $(NH_4)_6[TeMo_6O_{24}] \cdot 7H_2O$, and $(NH_4)_6[TeMo_6O_{24}] \cdot Te(OH)_6 \cdot 7H_2O$ single crystals and their deuterated analogues are studied to elucidate more information about the nature of vibration of the heteropolyanion and the effect of hydrogen bonding in these crystals.

[1] To whom correspondence should be addressed.

EXPERIMENTAL

$K_6[TeMo_6O_{24}] \cdot 7H_2O$ (abbreviated as KTMH) single crystals suitable for polarization studies were prepared by dissolving stoichiometric amounts of $K_6Mo_7O_{24} \cdot 4H_2O$ and H_6TeO_6 in water and allowing the solution to evaporate at room temperature (300 ± 3K) (4). $(NH_4)_6[TeMo_6O_{24}] \cdot 7H_2O$ (abbreviated as NTMH1) and $(NH_4)_6[TeMo_6O_{24}] \cdot Te(OH)_6 \cdot 7H_2O$ (abbreviated as NTMH2) were prepared in the same manner by dissolving stoichiometric amounts of $(NH_4)_6Mo_7O_{24} \cdot 4H_2O$ and telluric acid in water (4). Well-polished crystals with sides parallel to the crystallographic axes were used to record the Raman spectra in different orientations. The deuteration of the compounds was carried out by dissolving the title compounds repeatedly in heavy water and polycrystalline samples were used to record the spectra. Raman spectra were recorded using both a Dilor Z24 triple monochromator and a Spex 1401 double monochromator with a resolution better than 3 cm^{-1}. A Spectra Physics model 165 argon ion laser operating at an output of 200 mW for a 514.5 nm line was used as the excitation source. The infrared spectra were recorded on a Perkin–Elmer 577 spectrophotometer using KBr pellet technique.

FACTOR GROUP ANALYSIS

$K_6[TeMo_6O_{24}] \cdot 7H_2O$ crystallizes in the orthorhombic system with space group $Pcab$ (D_{2h}^{15}), having four molecules per Bravais unit cell (4). Molybdenum, potassium, and hydrogen atoms occupy general sites, whereas oxygen atoms are placed in general as well as C_i sites. The tellurium atom occupies the centrosymmetric site in KTMH. Factor group analysis by the correlation method developed by Fateley *et al.* gives the distribution of irre-

0022-4596/95 $12.00

ducible representation (8), excluding acoustic modes,

$$\Gamma_{KTMH} = 84A_g + 84B_{1g} + 84B_{2g} + 84B_{3g} + 90A_u + 89B_{1u} + 89B_{2u} + 89B_{3u}.$$

$(NH_4)_6[TeMo_6O_{24}] \cdot 7H_2O$ crystallizes in the orthorhombic system with space group $Pnaa$ (D_{2h}^{10}). There are four molecules per Bravais unit cell (4). Except for tellurium and oxygen, all atoms are in general sites. The tellurium atom occupies a centrosymmetric site while oxygen atoms are in C_1 and C_2 sites. Factor group analysis gives the distribution of irreducible representation, excluding acoustic modes, as

$$\Gamma_{NTMH1} = 121A_g + 122B_{1g} + 122B_{2g} + 121B_{3g} + 124A_u + 124B_{1u} + 124B_{2u} + 123B_{3u}.$$

$(NH_4)_6[TeMo_6O_{24}] \cdot Te(OH)_6 \cdot 7H_2O$ belongs to the monoclinic system with space group $A2/a$ (C_{2h}^6), having two formula units per Bravais unit cell (4). Oxygen atoms are placed in both C_1 and C_2 sites while all other atoms are at the general site C_1. Irreducible representation shows that 567 factor group modes of NTMH2, excluding acoustic modes, split into

$$\Gamma_{NTMH2} = 142A_g + 143B_g + 141A_u + 141B_u.$$

In all three crystals, the symmetry of the $[TeMo_6O_{24}]^{6-}$ ion is reduced from D_{3d} ($\bar{3}m$) to C_1, and this may lift the degeneracies of the normal modes. The six molybdenum atoms in the ion form a nearly perfect planar hexagon around the tellurium atom at the center and the average Te–Mo distance is 3.29 ± 0.01 Å (Fig. 1). These atoms lie near the center of seven octahedra which are formed by two sheets of 12 oxygen atoms, each positioned one over the other in close packing (4). In the anion, the MoO_6 octahedron has three different Mo–O bond lengths. Type I is between Mo and O_a atoms, linked to 2Mo + Te atoms with an average bond length of 2.294 Å, whereas in type II the Mo–O_b bond length is 1.939 Å, linked to 2Mo atoms. Finally, type III is between Mo and O_c, is linked to a single Mo atom, and has a bond length of 1.711 Å.

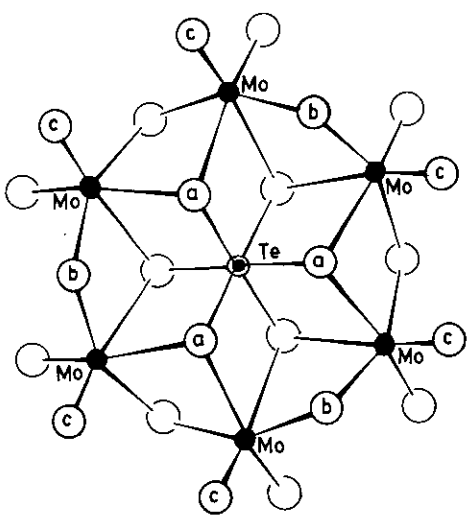

FIG. 1. Plan view of the hexamolybdotellurate anion $[TeMo_6O_{24}]^{6-}$.

In the complex anion, different groups of atoms can be isolated. Therefore, the assignments are made on the basis of the vibrations of MoO_6 and TeO_6 octahedra, NH_4 tetrahedra, and water molecules.

SPECTRAL ANALYSIS OF $K_6[TeMo_6O_{24}] \cdot 7H_2O$

MoO_6 Vibrations

For an MoO_6 ion having O_h symmetry, there are six fundamental vibrations, symmetric stretching mode $\nu_1(A_{1g})$, asymmetric stretching modes $\nu_2(E_g)$ and $\nu_3(F_{1u})$, asymmetric bending mode $\nu_4(F_{1u})$, symmetric bending mode $\nu_5(F_{2g})$, and inactive mode $\nu_6(F_{2u})$ (9–11).

In the crystal, the MoO_6 octahedral ions lose their O_h symmetry by the sharing of oxygen atoms with TeO_6 group. Since there are three different Mo–O distances and different O–Mo–O angles in the crystal, the spectrum is expected to be very complex with separate frequencies for the individual Mo–O distances and O–Mo–O angles (12, 13).

There are 24 MoO_6 units in the Bravais cell of KTMH and they occupy general sites. Table 1 gives the relationship between various symmetry species of O_h, C_1, and D_{2h} groups. According to group theoretical analysis, all of the vibrational modes become active in A_g, B_{1g}, B_{2g}, and B_{3g} polarizations of D_{2h} symmetry, as the octahedral MoO_6 ion goes to the C_1 site in the crystal. The polarizability tensor components of $\nu_1 MoO_6(O_h)$ are α_{xx}, α_{yy}, and α_{zz} (x, y, and z corresponding to the a, b, and c axes), and these components belong to the A_g species of the D_{2h} factor group (Table 2). Therefore, without any distortion of the MoO_6 ion, these modes appear in the Raman spectra in the A_g polarization of the crystal. But the distortion (14) of the ion leads to the appearance of this mode corresponding to the off-diagonal polarizability tensor components.

The polarized Raman bands observed in the 916 to 955 cm^{-1} region in all the orientations are split into three bands with different intensities (Figs. 2a and 2b). According to Hardcastle and Wachs, the short Mo–O bonds vibrate at higher frequencies (15). Therefore, the symmetric stretching vibrations of the terminal Mo–O_c bonds (1.711 Å) should give strong Raman peaks at a relatively high frequency. The intense bands in the 916 to 955 cm^{-1} region

TABLE 1
Correlation Scheme for the Internal Modes of MoO_6^{6-} and TeO_6^{6-} in $M_6[TeMo_6O_{24}] \cdot 7H_2O$ [M = K, NH_4], $z^B = 4$

	Free ion symmetry O_h		Site symmetry C_1	Factor group symmetry D_{2h}		
			MoO_6^{6-}			
24	A_{1g}	$(\nu_1)(\alpha_{xx} + \alpha_{yy} + \alpha_{zz})$		$(\alpha_{xx}, \alpha_{yy}, \alpha_{zz})$	A_g	45
48	E_g	$(\nu_2)(\alpha_{xx} + \alpha_{yy} - 2\alpha_{zz}, \alpha_{xx} - \alpha_{yz})$		(α_{xy})	B_{1g}	45
72	F_{2g}	$(\nu_5)(\alpha_{xy}, \alpha_{xz}, \alpha_{yy})$		(α_{xz})	B_{2g}	45
144	$2F_{1u}$	(ν_3, ν_4)	A	(α_{yz})	B_{3g}	45
72	F_{2u}	(ν_6)			A_u	45
					B_{1u}	45
					B_{2u}	45
					B_{3u}	45
			TeO_6^{6-}			
4	A_{1g}	$(\nu_1)(\alpha_{xx} + \alpha_{yy} + \alpha_{zz})$		$(\alpha_{xx}, \alpha_{yy}, \alpha_{zz})$	A_g	6
8	E_g	$(\nu_2)(\alpha_{xx} + \alpha_{yy} - 2\alpha_{zz}, \alpha_{xx} - \alpha_{yz})$	A_g	(α_{xy})	B_{1g}	6
12	F_{2g}	$(\nu_5)(\alpha_{xy}, \alpha_{xz}, \alpha_{yy})$		(α_{xz})	B_{2g}	6
24	$2F_{1u}$	(ν_3, ν_4)		(α_{yz})	B_{3g}	6
12	F_{2u}	(ν_6)			A_u	9
			A_u		B_{1u}	9
					B_{2u}	9
					B_{3u}	9

observed in all the polarization geometries are assigned to the terminal ν_sMo–O_c vibrations (16, 17). The intensity of this vibration is strongest in the $b(cc)a$ orientation. However, its appearance as triplet in all the polarization settings suggests the effect of correlation field splitting. In the infrared spectrum, two very strong bands are observed at 930 and 914 cm^{-1} in this region. These bands shift to lower wavenumbers in the deuterated compound. The asymmetric stretching vibrations of the Mo–O_c bonds are observed as weak bands in the Raman spectra while the infrared spectrum gives two strong bands at 889 and 879 cm^{-1}.

In the telluromolybdate anion, there are six Mo–O_b–Mo and Mo–O_a–Mo bridges with average Mo–O bond lengths

TABLE 2
Correlation Scheme for the Internal Modes of MoO_6^{6-} and TeO_6^{6-} in $(NH_4)_6[TeMo_6O_{24}] \cdot Te(OH)_6 \cdot 7H_2O$, $z^B = 2$

	Free ion symmetry O_h		Site symmetry C_1	Factor group symmetry C_{2h}		
			MoO_6^{6-}			
12	A_{1g}	$(\nu_1)(\alpha_{xx} + \alpha_{yy} + \alpha_{zz})$		$(\alpha_{xx}, \alpha_{yy}, \alpha_{zz}, \alpha_{xy})$	A_g	45
24	E_g	$(\nu_2)(\alpha_{xx} + \alpha_{yy} - 2\alpha_{zz}, \alpha_{xx} - \alpha_{yy})$		$(\alpha_{xz}, \alpha_{yz})$	B_g	45
36	F_{2g}	$(\nu_5)(\alpha_{xy}, \alpha_{xz}, \alpha_{yz})$	A		A_u	45
72	$2F_{1u}$	(ν_3, ν_4)			B_u	45
36	F_{2u}	(ν_6)				
			TeO_6^{6-}			
4	A_{1g}	$(\nu_1)(\alpha_{xx} + \alpha_{yy} + \alpha_{zz})$		$(\alpha_{xx}, \alpha_{yy}, \alpha_{zz}, \alpha_{xy})$	A_g	15
8	E_g	$(\nu_2)(\alpha_{xx} + \alpha_{yy} - 2\alpha_{zz}, \alpha_{xx} - \alpha_{yy})$		$(\alpha_{xz}, \alpha_{yz})$	B_g	15
12	F_{2g}	$(\nu_5)(\alpha_{xy}, \alpha_{xz}, \alpha_{yz})$	A		A_u	15
24	$2F_{1u}$	(ν_3, ν_4)			B_u	15
12	F_{2u}	(ν_6)				

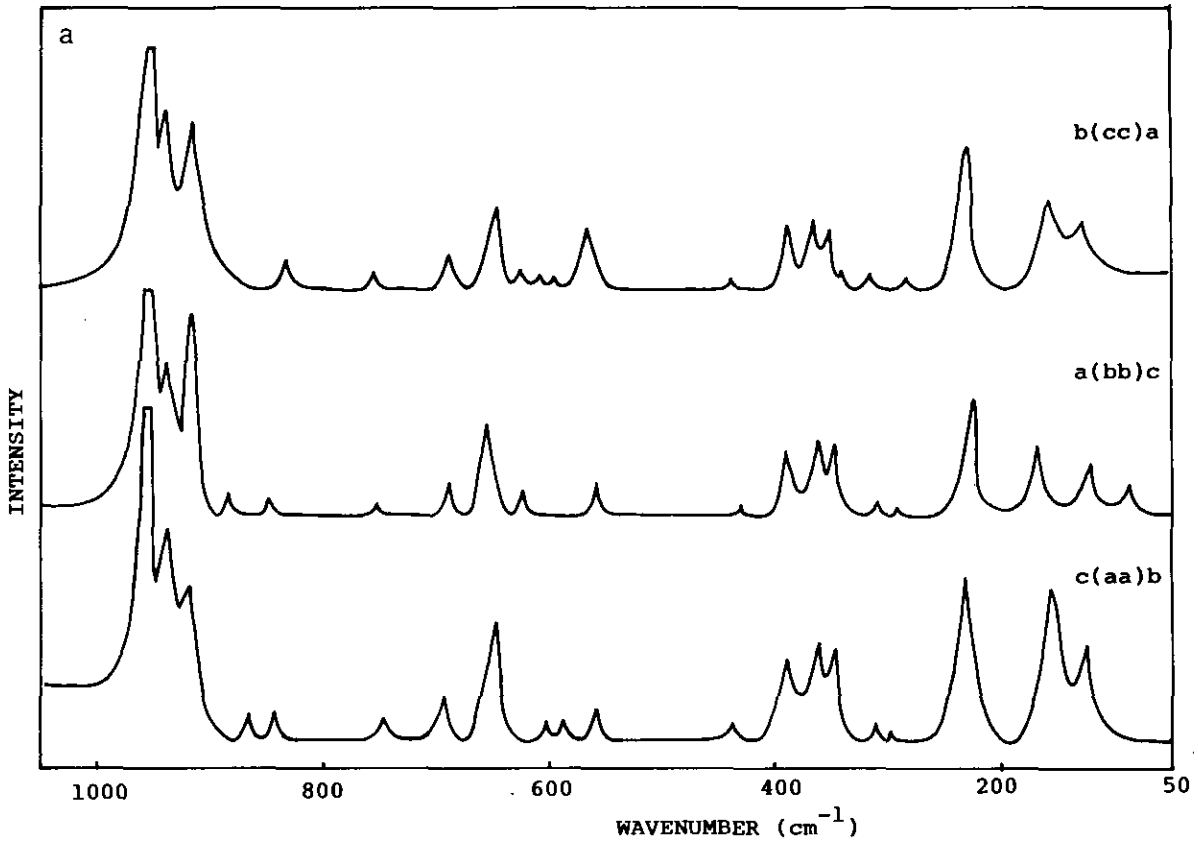

FIG. 2a. Raman spectra of $K_6[TeMo_6O_{24}] \cdot 7H_2O$ in the 50–1000 cm^{-1} region for *c(aa)b*, *a(bb)c*, and *b(cc)a* orientations.

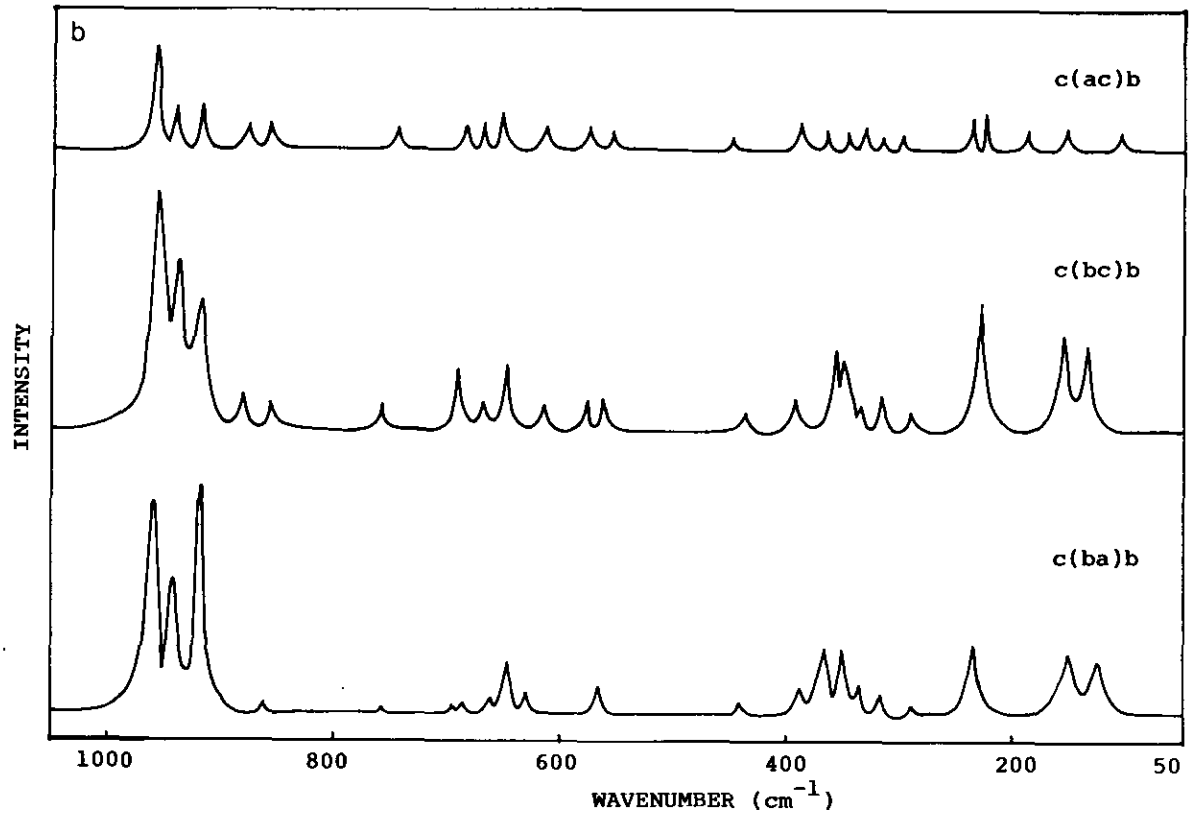

FIG. 2b. Raman spectra of $K_6[TeMo_6O_{24}] \cdot 7H_2O$ in the 50–1000 cm^{-1} region for *c(ba)b*, *c(bc)b*, and *c(ac)b* orientations.

of 1.934 and 2.294 Å, respectively. Analysis of the spectra of many polymolybdates has shown that vibrations of bridging bonds occur at a frequency lower than those of terminal bonds (18, 19). On the basis of the observed polarization effects and Hardcastle's criteria (15), the polarized Raman bands observed around the 680 to 695 cm^{-1} region are assigned to the symmetric stretching vibrations of Mo–O_b–Mo bridges. Even though these Raman bands are observed in all polarizations, the intensities of these bands are much lower than in the $Mo_7O_{24}^{6-}$ species (16). The corresponding IR bands appear as two medium-intensity bands at 691 and 680 cm^{-1}. On deuteration, only one band is obtained in the IR while no band is observed in the Raman spectrum.

As expected, the asymmetric stretching vibrations of Mo–O_b–Mo bridges are very weak and bands are observed only for the off-diagonal polarization tensors (Table 3). The infrared spectrum gives a medium-intensity band at 666 cm^{-1} in this region.

The polarized Raman bands observed in the 346 to 365 cm^{-1} region are assigned to the symmetric stretching vibrations of Mo–O_a–Mo bridges with long Mo–O_a bond length (2.254 Å). Deuteration does not bring a noticeable frequency shift to these bands. The asymmetric stretching vibrations of Mo–O_a–Mo bridges may be obscured by the symmetric bending modes of TeO_6 group. These vibrations cannot be clearly assigned in both Raman and IR spectra.

The symmetric deformation vibrations of the six V-shaped O_c–Mo–O_c groups on the outer edge of the $[TeMo_6O_{24}]^{6-}$ anion with an average bond angle of 106° are observed as a medium-intensity broad band around 560 cm^{-1} in all the polarization settings except $c(ac)b$, where only a weak band is observed. The bands observed for the asymmetric bending vibrations of O_c–Mo–O_c groups are weak in the Raman spectra, while two bands, one an intense band and the other medium intense, at 470 and 431 cm^{-1}, respectively, are obtained in the IR spectrum.

A strong broad band observed in all orientations of the crystal around 220–235 cm^{-1} in the Raman spectra is assigned to the Mo–O–Mo deformations. The Mo–O_a–Mo bridge in the telluromolybdate anion is more angularly distorted than the Mo–O_b–Mo bridge (4). All such vibrations overlap to give a broad band in this region for all polarizations and also in the Raman spectrum of the deuterated compound.

The symmetric stretching vibrations of the terminal Mo–O_c bonds are found to decrease toward lower wavenumber regions on deuteration in both Raman and IR spectra. This can happen as the distortion of MoO_6 octahedra is reduced due to the changes in the hydrogen bond structure when the hydrogen atom is replaced by a deuterium atom.

TeO_6 Vibrations

The stretching and bending modes of TeO_6 octahedron usually occur in the regions 550 to 750 cm^{-1} and 350 to 450 cm^{-1}, respectively (20, 21). The polarized Raman bands observed in the ca. 650 cm^{-1} region in all the orientations are assigned to the symmetric stretching $\nu_1(A_{1g})$ vibrations of the TeO_6 ion. The assignment of ν_2 and ν_3 modes is done on the basis of their relative intensities in the IR and Raman spectra and by taking into account the fact that ν_2 is normally Raman active and that ν_3 is infrared active. However, the inactive modes can appear as weak bands. In the Raman spectra, very weak bands are observed for the ν_3 mode in a few of the polarizations. The ν_2 mode also gives a medium-intensity band in the infrared spectrum. The deformation vibrations ν_4 and ν_5 are also assigned on the basis of their intensities in the spectra (22).

In the factor group analysis, the TeO_6 group is situated at the centrosymmetric site and hence the IR and Raman bands are expected to obey the mutual exclusion principle. The IR-inactive ν_1, ν_2, and ν_5 bands are observed in the IR spectra of both protonated and deuterated compounds. The Raman-inactive ν_4 mode is observed in all the polarizations of the Raman spectra. As the mutual exclusion principle is not obeyed, the TeO_6 ion can be inferred to be occupying a symmetry lower than C_i. This is further confirmed by the appearance of Raman- and IR-inactive ν_6 mode (23).

Water Vibrations

A number of bands are observed with frequencies considerably shifted from the free state values of water molecules, indicating the presence of hydrogen bonds of various strengths (24, 25). In the Raman spectrum of KTMH, four weak bands are observed in the 2975 to 3480 cm^{-1} region. These bands are assigned to the symmetric (ν_1) and asymmetric (ν_3) stretching modes of water molecules. The infrared spectrum of the polycrystalline sample shows a strong broad band in the 2900 to 3480 cm^{-1} region with two humps at 3360 and 2962 cm^{-1}. The weak bands obtained in the 2300 to 2600 cm^{-1} region in the infrared spectrum of the deuterated compound (KTMD) are assigned to the D_2O stretching modes (Fig. 3). In the Raman spectrum, the stretching modes of D_2O are also obtained in this region.

The in-plane bending vibration of H_2O is observed as a strong band in the IR spectrum at 1618 cm^{-1} and as a weak one at 1641 cm^{-1}. The corresponding bands in the Raman spectra are very weak. In the deuterated compound, these modes are shifted to the 1240 to 1300 cm^{-1} region in both the IR and Raman spectra. The number of bands in the stretching and bending region indicates the presence of two different types of water molecules in the crystal.

TABLE 3
Spectral Data (cm^{-1}) and Band Assignments of $K_6[TeMo_6O_{24}] \cdot 7H_2O/D_2O$

$K_6[TeMo_6O_{24}] \cdot 7H_2O$							$K_6[TeMo_6O_{24}] \cdot 7D_2O$		
Raman									
b(cc)a A_g	*a(bb)c* A_g	*c(aa)b* A_g	*c(ba)b* B_{1g}	*c(ac)b* B_{2g}	*c(bc)b* B_{3g}	IR	Raman	IR	Assignments
3441 w	3458 wbr	3439 wbr 3408 w	3479 w	3456 wbr	3439 wbr	3480– 2900 sbr		3420– 2600 sbr	
3213 wbr	3381 wbr		3231 wbr	3142 wbr	3335 w		3337 wbr		ν_3, ν_1 H_2O
3101 w	3077 mbr	3095 wbr	3136 w	3097 wbr	3216 wbr		3192 wbr		
2976 vw	3024 wbr	2994 wbr	2981 w	2991 wbr	3011 wbr				
							2486 w		
							2386 w	2300–	ν_3, ν_1 D_2O
							2338 w	2040 mbr	
1647 w	1617 w	1631 w	1642 w	1642 w	1639 wbr	1641 w			
1614 wbr	1609 w	1598 w	1634 wbr	1598 w	1608 w	1618 m	1628 vw	1608 m	ν_2 H_2O
							1258 w	1298 w	
							1244 w	1271 w	ν_2 D_2O
						1085 mbr		1077 mbr	combination
952 vs	954 vs	955 vs	954 s	955 s	955 vs				
940 s	939 m	938 s	939 m	939 m	937 s	930 vs	938 s		
916 s	917 s	919 mbr	917 vs	917 m	918 m	914 vs	910 mbr	908 s	ν_s Mo–O_c
							888 mbr		
	886 w	868 w	862 wbr	876 w	881 w	889 s	866 w	873 s	
834 vw	848 w	844 w		855 w	854 w	879 s			ν_{as} Mo–O_c
756 wbr	752 wbr	748 wbr	756 wbr	743 wbr	758 wbr				ν_r H_2O
		694 mbr	691 vw		690 wbr	691 m		699 m	
688 mbr	689 wbr		688 wbr	683 w		680 m	686 vw		ν_s Mo–O_b–Mo
			661 w	668 w	667 wbr	666 m		666 m	ν_{as} Mo–O_b–Mo
646 mbr	653 mbr	647 s	645 mbr	650 w	647 m	645 m	648 w	639 m	ν_1 TeO_6
626 w	627 w		629 w			637 m	628 w		
608 w		604 w		612 wbr	614 vw			614 m	ν_2 TeO_6
596 w		586 w		572 w	576 vw	590 s		579 m	ν_3 TeO_6
564 mbr	559 mbr	560 mbr	565 mbr	552 vw	563 m		548 w		
						528 m		518 m	δ_s O_c–Mo–O_c
						470 m		461 w	
437 wbr	430 w	438 w	439 vw	448 vw	436 w	431 s	444 vw	425 mbr	δ_{as} O_c–Mo–O_c
387 mbr	389 mbr	390 mbr	388 mbr	387 w	391 mbr	389 w	392 w	397 vw	ν_4 TeO_6
365 mbr	360 m	363 s	364 mbr	364 w	354 m	368 w	366 vw	360 vw	
350 mbr	348 m	347 m	350 m	346 vw	348 m	350 m	356 mbr	338 vw	ν_s Mo–O_a–Mo
338 vw			335 w	332 w	334 w				ν_{as} Mo–O_a–Mo
314 wbr	311 w	312 w	317 wbr	314 vwbr	314 m	326 m		312 w	ν_5 TeO_6
282 w	293 w	298 w	291 w	298 w	290 wbr	258 w			ν_6 TeO_6
			235 sbr	234 m			238 mbr		
227 sbr	226 sbr	229 sbr		223 m	229 sbr	229 m	221 w		δ Mo–O–Mo
				188 w					
156 mbr	164 s	156 s	151 mbr	153 wbr	154 s		162 wbr		
127 mbr	122 w	128 m	126 mbr		132 s				External modes
	88 w			104 w					

Note. Relative intensities: vs, very strong; s, strong; m, medium; w, weak; vw, very weak; br, broad; r, rocking.

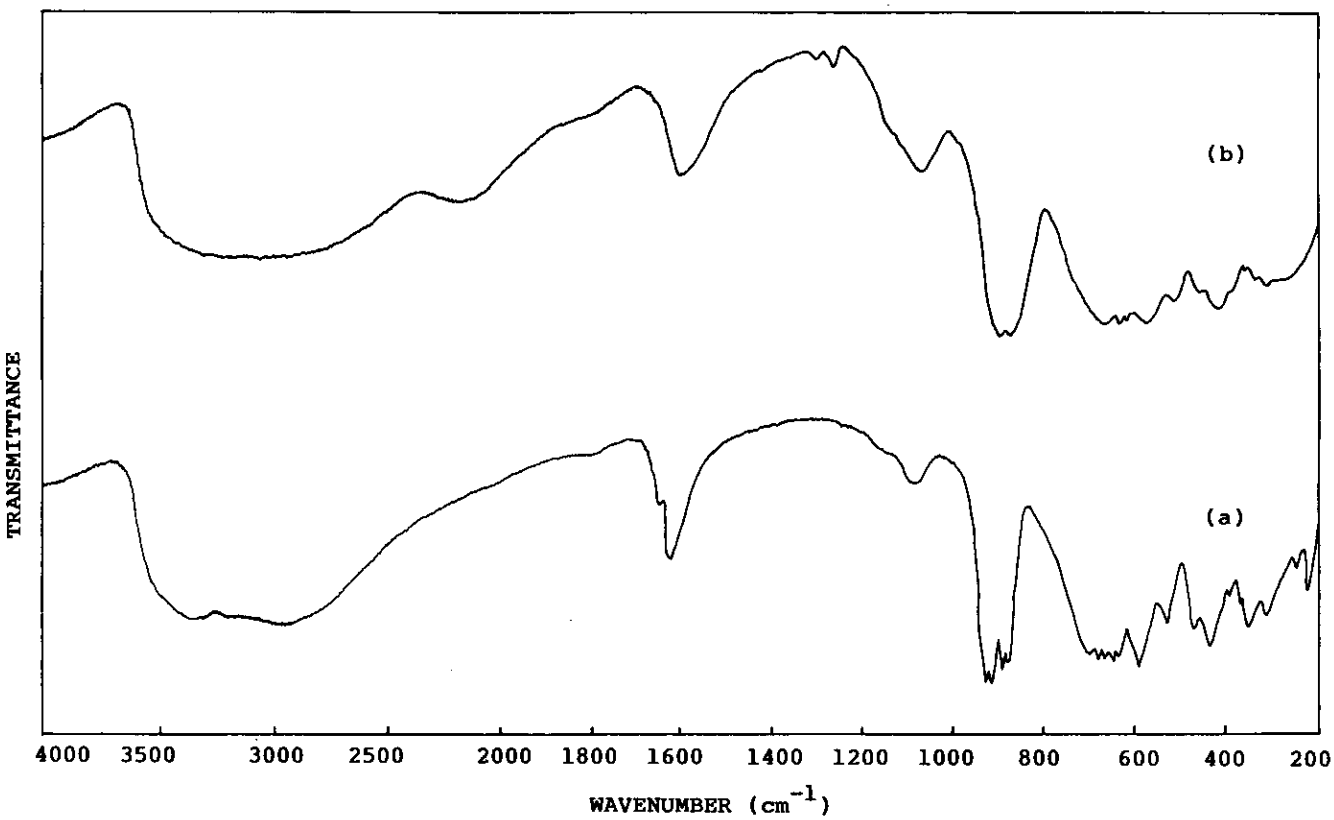

FIG. 3. Infrared spectra of (a) $K_6[TeMo_6O_{24}] \cdot 7H_2O$ and (b) $K_6[TeMo_6O_{24}] \cdot 7D_2O$ in the 200–4000 cm^{-1} region.

Vibrational modes of water cannot be clearly identified as they fall in the internal mode region of MoO_6 and TeO_6 ions. However, rocking modes of H_2O are assigned in the Raman spectra as weak broad bands.

SPECTRAL ANALYSIS OF $(NH_4)_6[TeMo_6O_{24}] \cdot 7H_2O$

MoO_6 Vibrations

The 24 MoO_6 units in the Bravais cell of NTMH1 occupy general sites. Since the relationships between the various symmetry species of O_h, C_1, and D_{2h} groups are identical (Table 1), the distortion-induced activity can be explained in the same way as that in KTMH. Vibrational assignments of the MoO_6 modes are also similar to those of the MoO_6 ions in KTMH (Table 4). However, the symmetric stretching vibrations of terminal Mo–O_c bonds are obtained at lower wavenumbers than in the potassium compound. No significant reduction in wavenumbers is observed in this compound for the ν_sMo–O_c vibrations on deuteration.

The symmetric and asymmetric vibrations of the Mo–O_b–Mo bridges are observed in the 675 to 700 cm^{-1} region in the Raman spectra with weak intensity while the corresponding infrared spectrum gives a strong broad absorption ranging from 642 to 672 cm^{-1}.

The symmetric stretching vibrations of Mo–O_a–Mo bridges give a strong band around 350 cm^{-1} in both IR and Raman spectra.

TeO_6 Vibrations

The nondegenerate and doubly degenerate stretching vibrations of TeO_6 groups (ν_1 and ν_2) are observed as very weak bands in the Raman spectra of NTMH1 crystal (Figs. 4a and 4b). The bands are present only in the $a(bb)c$, $c(aa)b$, $c(ac)b$, and $c(bc)b$ orientations. The triply degenerate asymmetric stretching (ν_3) mode gives Raman bands in all orientations. The assignment of this mode is supported by the strong IR band observed at 597 cm^{-1}. The bending vibrations of TeO_6 groups are also assigned. TeO_6 groups occupy a symmetry lower than that of C_i in NTMH1 as observed in KTMH.

NH_4 Vibrations

The normal modes of vibration of a free NH_4 ion under T_d symmetry have frequencies at 3033, 1689, 3134, and 1397 cm^{-1} for $\nu_1(A_1)$, $\nu_2(E)$, $\nu_3(F_2)$, and $\nu_4(F_2)$ modes. Of these, ν_1 and ν_2 are active only in Raman while ν_3 and ν_4 are active both in Raman and IR. Since the NH_4^+ ions occupy sites of lower symmetry than those of the free ion, anisotropic crystal fields may remove degeneracies

TABLE 4
Spectral Data (cm^{-1}) and Band Assignments of $(NH_4)_6[TeMo_6O_{24}] \cdot 7H_2O/D_2O$

$(NH_4)_6[TeMo_6O_{24}] \cdot 7H_2O$							$(ND_4)_6[TeMo_6O_{24}] \cdot 7D_2O$		
Raman									
b(cc)a A_g	*a(bb)c* A_g	*c(aa)b* A_g	*c(ba)b* B_{1g}	*c(ac)b* B_{2g}	*c(bc)b* B_{3g}	IR	Raman	IR	Assignments
3477 w 3407 mbr	3472 w 3417 wbr	3458 w	3483 vw 3409 wbr	3444 wbr	3413 mbr	3520– 3300 sbr		3500– 3000 mbr	ν_3, ν_1 H_2O
3313 w 3304 vw	3381 w 3310 w	3384 w 3314 vw	3299 wbr	3322 w 3298 w	3351 w 3274 wbr		3348 w 3274 wbr		
3228 mbr 3162 w 3079 mbr	3076 mbr	3241 w 3076 mbr	3162 wbr 3082 vw 3034 wbr	3172 wbr 3024 w	3229 w 3078 w 3026 w	3180– 3040 vs	3114 wbr		ν_3 NH_4^+
2954 w		2963 w	2963 vw	2967 wbr 2946 mbr	2968 wbr	2982 m	2953 vw		ν_1 NH_4^+
							2422 wbr 2382 wbr	2390 wbr 2320 wbr	ν_3, ν_1 D_2O
							2264 wbr	2288 w	ν_3, ν_1 ND_4^+
	2278 w	2288 w	2282 w	2280 w	2290 w	2262 vw			$\nu_2 + \nu_6$ NH_4^+
1916 vw	1939 vw	1908 vw	1929 wbr	1922 w	1930 wbr	1928 w			$\nu_4 + \nu_6$ NH_4^+
1767 mbr 1714 w 1698 w	1772 vw 1719 wbr	1762 wbr 1703 wbr	1718 w 1694 vw	1704 w 1682 wbr	1716 wbr 1704 w				ν_2 NH_4^+
1603 vw	1580 w	1604 w	1620 w	1620 wbr 1595 wbr	1622 w 1612 w	1641 mbr	1064 wbr	1570 mbr	ν_2 H_2O
1426 w	1408 w	1410 wbr	1421 wbr	1438 w	1408 w	1445 w 1385 s	1374 w	1381 s	ν_4 NH_4^+
							1273 wbr	1258 wbr	ν_2 D_2O
						1106 wbr			Combination
							1092 w	1130 w 1080 w	ν_2, ν_4 ND_4^+
936 vs 907 vs 896 s	935 vs 904 s 892 s	936 vs 905 m 893 vs	936 vs 908 m 894 m	936 vs 906 s 893 m	936 s 907 m 892 m	910 vs 901 s	937 vs 906 m 895 s	910 s	ν_s Mo–O_c
864 w 845 w	864 w 839 w	839 w	871 w 849 vw	878 w 828 w	870 w 838 w	874 vs 860 vs	868 wbr	871 vs	ν_{as} Mo–O_c
688 m 682 w	688 w 675 w	697 m	690 vw	687 vw	688 vw	672– 642 sbr	682 vwbr	680– 635 sbr	ν_s Mo–O_b–Mo, ν_{as} Mo–O_b–Mo
	611 wbr	614 w		606 vw	630 wbr 607 vw		637 w 613 vw		ν_1, ν_2 TeO_6
586 w	582 wbr	598 w 589 w	588 mbr	592 w 584 w	588 wbr	597 s	594 wbr	590 sbr	ν_3 TeO_6
564 w 558 m	563 mbr 522 mbr	562 mbr 525 vw	566 w 509 w	554 mbr 523 m	561 mbr	526 m	561 mbr 526 mbr	540 mbr	δ_s O_c–Mo–O_c
452 w 438 w	436 wbr	448 w	453 wbr	451 w 414 w	448 vwbr 437 vw	448 s 441 s	411 vwbr 391 wbr	452– 397 mbr	δ_{as} O_c–Mo–O_c
389 m	388 sbr	388 mbr	387 mbr	387 mbr	386 wbr				ν_4 TeO_6

TABLE 4—*Continued*

$(NH_4)_6[TeMo_6O_{24}]\cdot 7H_2O$							$(ND_4)_6[TeMo_6O_{24}]\cdot 7D_2O$		
Raman									
b(*cc*)*a* A_g	*a*(*bb*)*c* A_g	*c*(*aa*)*b* A_g	*c*(*ba*)*b* B_{1g}	*c*(*ac*)*b* B_{2g}	*c*(*bc*)*b* B_{3g}	IR	Raman	IR	Assignments
354 sbr	348 sbr	350 sbr	353 sbr	350 mbr	358 mbr	346 s	352 mbr	339 wbr	ν_s Mo–O_a–Mo
	326 w	322 wbr			332 wbr				ν_{as} Mo–O_a–Mo,
307 w	309 w	315 mbr	316 w	310 wbr	310 wbr	314 w		302 w	ν_5 TeO_6
288 w	284 w	274 wbr		268 w		282 vw		282 vw	ν_6 TeO_6
224 sbr	226 sbr	223 vsbr	239 sbr	225 sbr	222 sbr	248 w	222 sbr	240 w	δ Mo–O–Mo
189 mbr	178 mbr	184 mbr	194 wbr	183 wbr	186 mbr		184 wbr		
149 m	138 m	136 w	140 mbr	146 wbr	161 w		140 wbr		External
					138 vw				modes
105 m	107 mbr	100 mbr	111 m	103 mbr	101 m		114 m		
					63 w				

of normal modes and allow inactive modes to become active (26, 27).

The assignments of the different vibrational modes of the NH_4^+ ion are given in Table 4. The Raman-active ν_1 mode is observed in the 2945 to 2969 cm^{-1} region. Even though IR inactive, a medium-intensity band is observed at 2982 cm^{-1} for this mode. As expected, the degeneracy of the ν_2 and ν_3 modes of NH_4^+ ion is completely lifted in

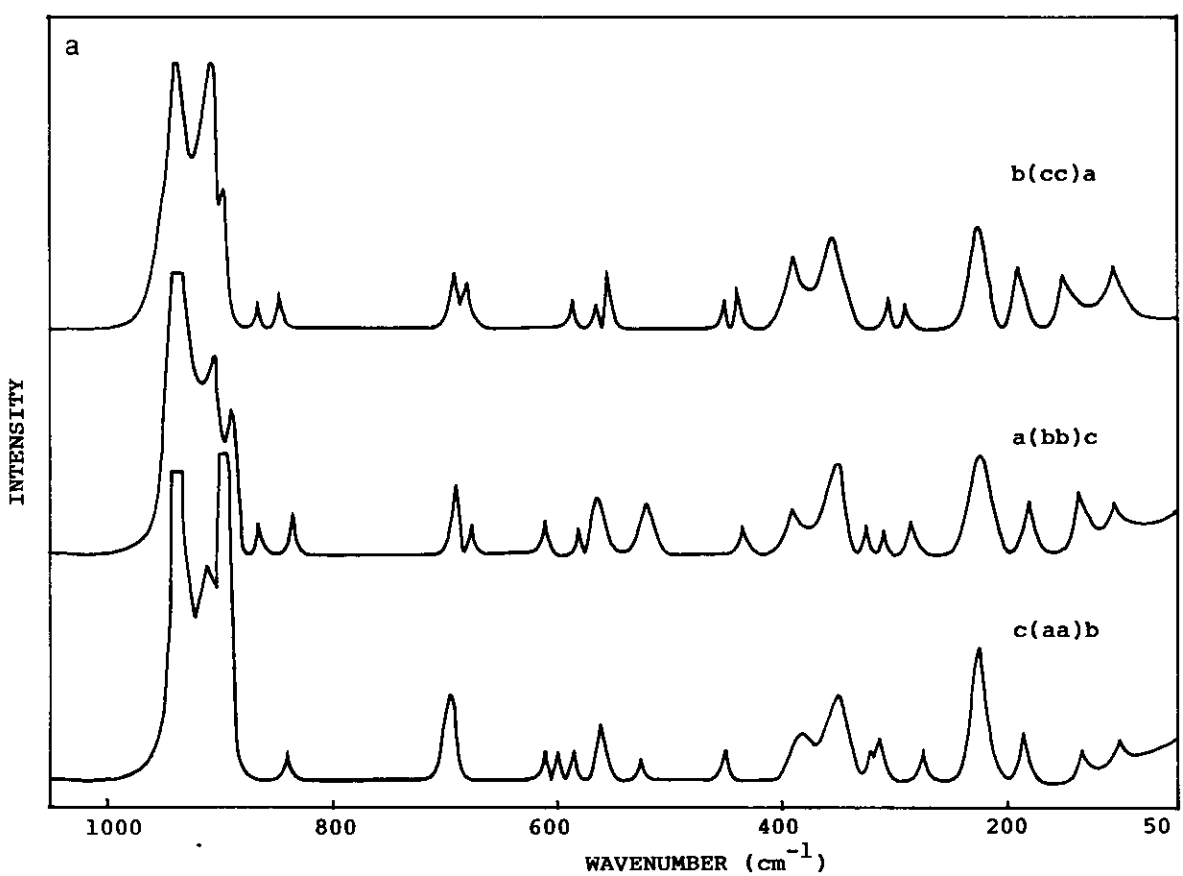

FIG. 4a. Raman spectra of $(NH_4)_6[TeMo_6O_{24}]\cdot 7H_2O$ in the 50–1000 cm^{-1} region for *c*(*aa*)*b*, *a*(*bb*)*c*, and *b*(*cc*)*a* orientations.

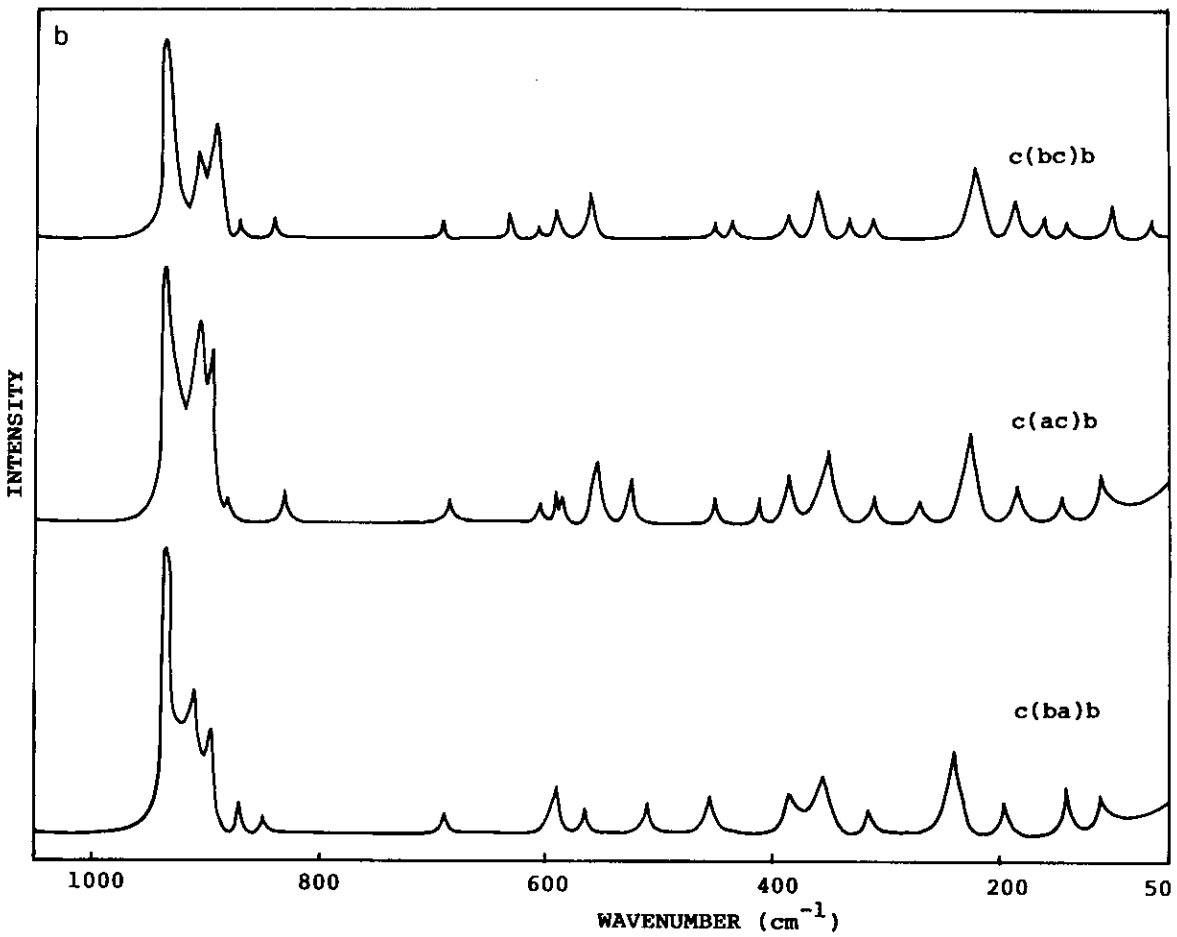

FIG. 4b. Raman spectra of $(NH_4)_6[TeMo_6O_{24}] \cdot 7H_2O$ in the 50–1000 cm^{-1} region for the *c(ba)b*, *c(ac)b*, and *c(bc)b* orientations.

NTMH1. However, the ν_4 mode retains its degeneracy in the Raman spectra.

In hydrogen-bonded inorganic systems, the observation of combinations of bending modes (ν_2, ν_4) with the internal rotation mode ν_6 indicates that the ion does not rotate freely in the crystalline lattice. In NTMH1, the $\nu_4 + \nu_6$ vibration is observed as a weak band in all of the polarization settings. The corresponding infrared band is obtained at 1928 cm^{-1}. The combination bands due to ν_2 and ν_6 are also observed in the Raman and IR spectra of NTMH1 except in the *b(cc)a* orientation (Fig. 4c). Appearance of these bands indicates that the NH_4^+ ion does not rotate freely in the crystalline lattice (28–30). The ν_sMo–O_c bands are observed at lower wavenumbers than in KTMH, indicating the formation of hydrogen bonds also with NH_4^+ ions in NTMH1 crystal.

On deuteration, the symmetric stretching vibrations of NH_4^+ ions are shifted to 2264 cm^{-1} corresponding to an isotopic shift ratio of 1.30. This is found to be lower than the free state value (31) of 1.355, indicating that N–H $\cdots$ O bonds form an asymmetric potential in NTMH1 crystal (32) (Fig. 5).

Water Vibrations

Multiple bands present in the stretching region of water in the Raman spectra with weak intensity in the 3274 to 3483 cm^{-1} region indicate the presence of hydrogen bonds of various strengths. In the IR spectrum, water bands give a strong broad absorption in the 3300 to 3520 cm^{-1} region. On deuteration, the stretching modes of water molecules are shifted toward the low wavenumber region and two weak broad bands are observed at 2422 and 2382 cm^{-1} in the Raman spectra. The infrared spectrum also gives two weak bands in this region. Only one broad band of medium intensity is observed in the bending mode region of water in the IR spectrum of NTMH1. Therefore it is difficult to identify the distinct types of water molecules observed in KTMH.

SPECTRAL ANALYSIS OF $(NH_4)_6[TeMo_6O_{24}] \cdot Te(OH)_6 \cdot 7H_2O$

MoO_6 Vibrations

The 12 MoO_6 units in NTMH2 occupy the general sites. Group theoretical analysis predicts that all the vibrational

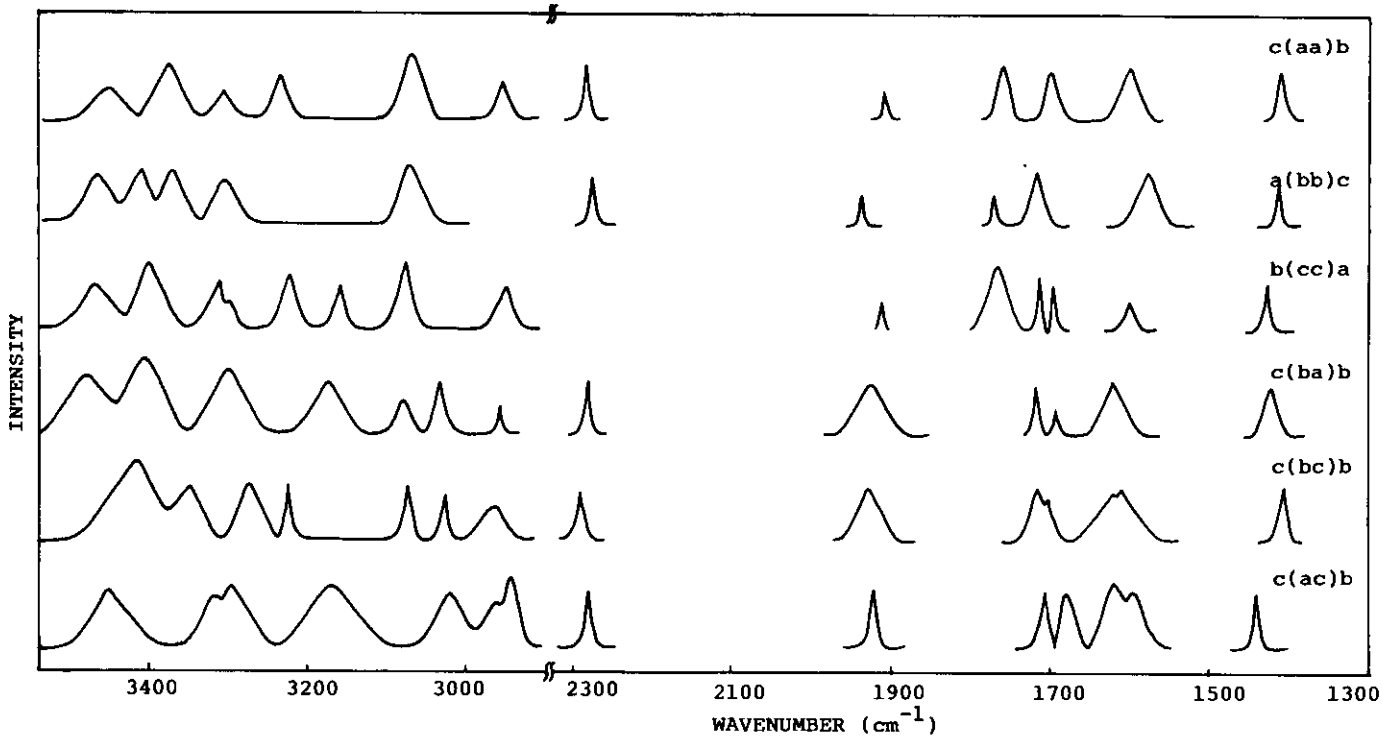

FIG. 4c. Raman spectra of $(NH_4)_6[TeMo_6O_{24}]\cdot 7H_2O$ in the 1300–3600 cm^{-1} region for *c(ac)b*, *c(bc)b*, *c(ba)b*, *b(cc)a*, *a(bb)c*, and *c(aa)b* orientations.

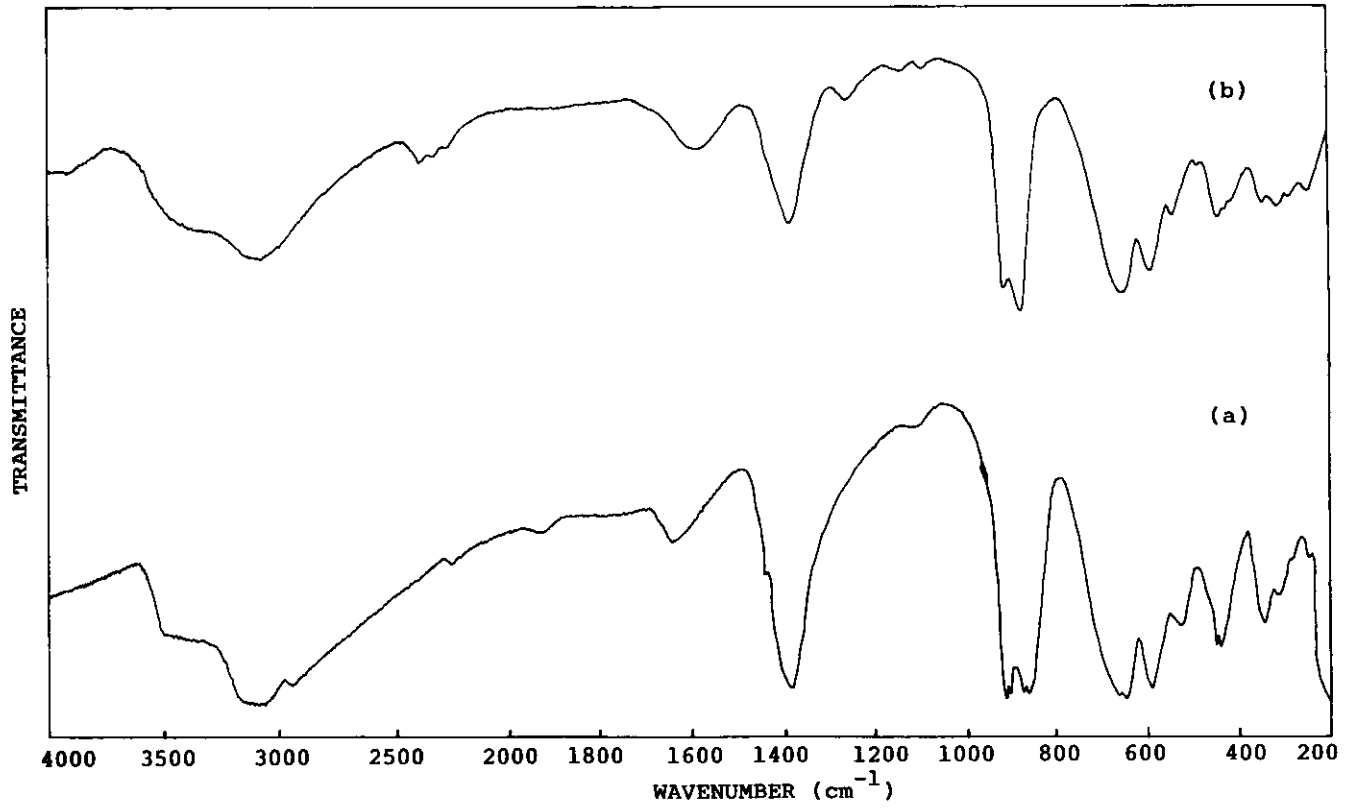

FIG. 5. Infrared spectra of (a) $(NH_4)_6[TeMo_6O_{24}]\cdot 7H_2O$ and (b) $(ND_4)_6[TeMo_6O_{24}]\cdot 7D_2O$ in the 200–4000 cm^{-1} region.

modes become active in the A_g and B_g polarizations as the octahedral MoO_6 ion goes to the C_1 site in the crystal of C_{2h} symmetry (Table 2). According to Bhattacharjee (14), the distortion-induced activity will lead to the appearance of ν_1 mode in B_g polarizations. From the correlation table it can be seen that ν_1 mode is active in B_g species also. This is due to the lowering of symmetry of the MoO_6 ion from O_h to C_1, which contributes α_{xz} and α_{yz} components.

The polarized Raman bands observed in the 891 to 939 cm^{-1} region are attributed to the symmetric stretching vibrations of the terminal Mo–O_c bonds. The intensity of these vibrations is found to be comparatively less than that of the other two crystals (Fig. 6a). The asymmetric stretching vibrations of Mo–O_c bonds give rise to strong IR bands at 889 and 871 cm^{-1} while the Raman spectra in this region give only a weak band in the *a(bb)c* orientation. The symmetric stretching vibrations of Mo–O_b–Mo bridges give weak Raman band except in the *a(ca)c* orientation. However, a strong IR band at 660 cm^{-1} is observed corresponding to the asymmetric stretching vibrations of these bridged bonds. The ν_sMo–O_a–Mo bridge modes are also obtained similar to those in NTMH1 crystal.

TeO_6 Vibrations

Even though one may expect strong Raman peaks for the stretching region of TeO_6 groups, no characteristic bands of the stretching vibrations (ν_1 and ν_2) are observed in the IR and Raman spectra of NTMH2 crystal. Apart from the central TeO_6 octahedron, there is one more $Te(OH)_6$ group attached to NTMH2 crystal. The telluric acid octahedra are firmly bound to the $[TeMo_6O_{24}]^{6-}$ group by hydrogen bonds of lengths 2.59, 2.61, and 2.63 Å,

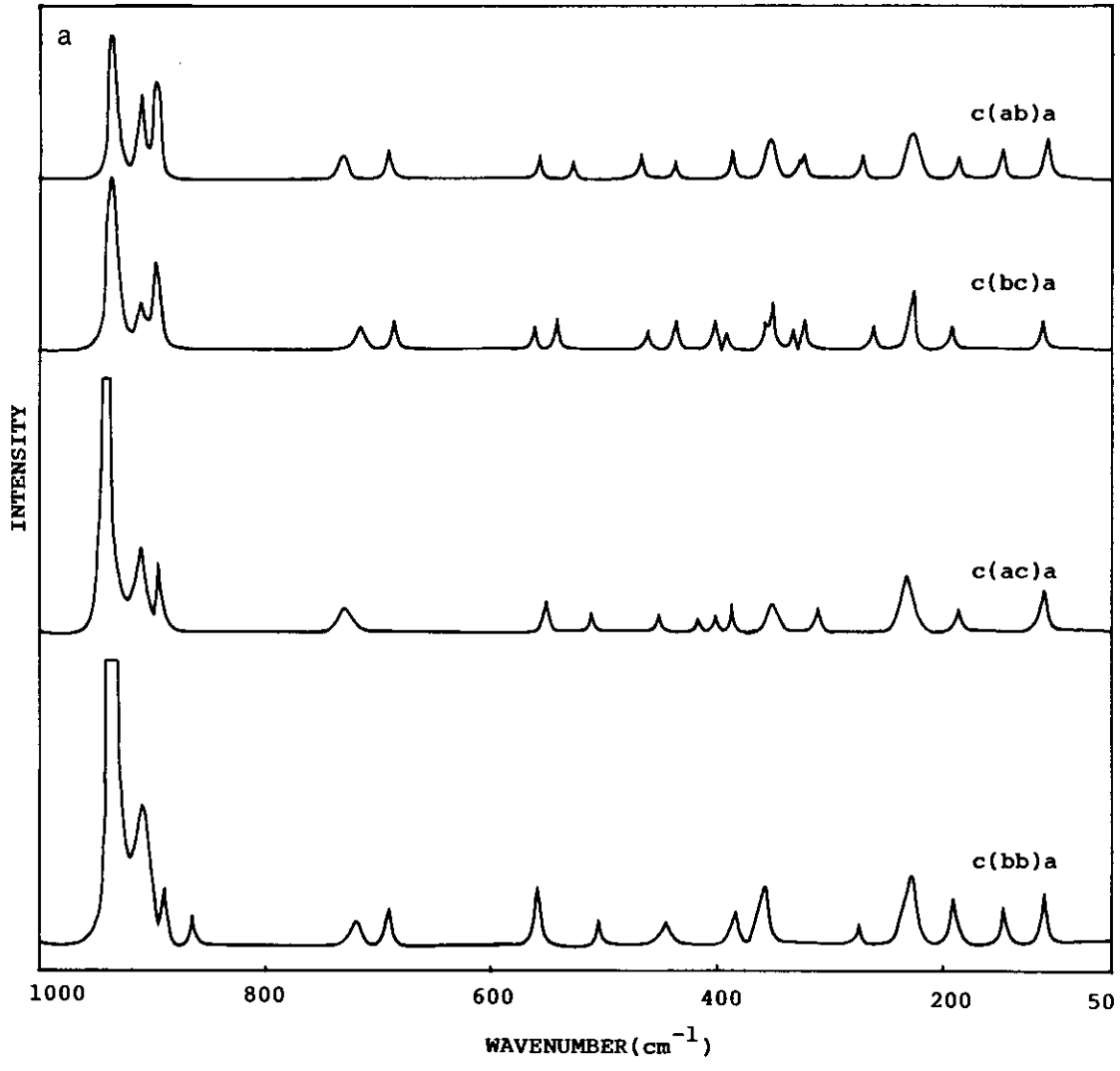

FIG. 6a. Raman spectra of $(NH_4)_6[TeMo_6O_{24}] \cdot Te(OH)_6 \cdot 7H_2O$ in the 50–1000 cm^{-1} region for the *c(bb)a*, *c(ac)a*, *c(bc)a*, and *c(ab)a* orientations.

respectively. Thermal parameter studies (4) also reveal that the central octahedron, TeO_6, of the hexamolybdotellurate group has the least amount of motion, while the tellurium atom at the center of the telluric acid molecule has somewhat greater motion. In both groups the thermal motion increases with the distance from the center. Moreover, the central TeO_6 octahedron is considerably flattened, with the upper and lower O···O distances consisting of unshared octahedral edges averaging 2.82 Å and transverse O···O distances consisting of shared edges averaging 2.64 Å. This can restrict the motion of the TeO_6 group, leading to a reduction in intensity of the TeO_6 modes. The observed internal modes of TeO_6 ions are assigned and the results are compiled in Table 5.

The stretching and bending vibrations of the terminal and bridging bonds of all three crystals (KTMH, NTMH1, and NTMH2) agree with the different Mo–O bond lengths predicted in the structural data. The bands of MoO_6 and TeO_6 ions reveal the existence of a $[TeMo_6O_{24}]^{6-}$ heteropolyanion in all three crystals, as suggested by Evans.

TABLE 5
Spectral Data (cm^{-1}) and Band Assignments of $(NH_4)_6[TeMo_6O_{24}] \cdot Te(OH)_6 \cdot 7D_2O$

$(NH_4)_6[TeMo_6O_{24}] \cdot Te(OH)_6 \cdot 7H_2O$					$(ND_4)_6[TeMo_6O_{24}] \cdot Te(OH)_6 \cdot 7D_2O$		
Raman							
c(bb)a A_g	*c(ab)a* A_g	*c(ac)a* B_g	*c(bc)a* B_g	IR	Raman	IR	Assignments
3497 wbr	3497 wbr	3483 wbr	3491 wbr	3524–		3520–	
3458 wbr	3470 w	3472 wbr		3300 sbr		2820 sbr	
3364 wbr	3412 wbr	3419 wbr	3362 wbr		3392 w		ν_3, ν_1 H_2O
	3309 wbr	3309 wbr	3308 wbr		3352 wbr		
3254 wbr			3268 wbr		3157 w		
3119 w				3280–			
3061 w	3042 w	3046 w	3047 w	2922 sbr			ν_3 NH_4^+
2942 w	2979 w	2980 wbr	2967 w				
2924 w	2930 w	2928 w	2911 wbr				ν_1 NH_4^+
					2387 w	2474 w	
					2348 w	2398 w	ν_3, ν_1 D_2O
2268 w	2290 w	2253 w	2252 w	2260 w			$\nu_2 + \nu_6$ NH_4^+
					2291 wbr	2160 w	ν_3, ν_1 ND_4^+
1951 w							
1931 w	1930 w	1926 w	1928 w	1931 vw	1931 vw		$\nu_4 + \nu_6$ NH_4^+
1738 w	1738 w	1738 w					
1717 wbr	1718 w	1717 wbr	1714 wbr				ν_2 NH_4^+
	1622 wbr		1627 wbr				
1606 wbr		1606 wbr	1608 vw	1609 mbr	1601 vwbr		ν_2 H_2O
1581 wbr	1596 w	1577 wbr		1590 mbr		1586 mbr	
1437 w	1434 w	1402 w	1436 w				
1384 w	1401 w	1381 w	1411 w	1378 s	1396 vw	1378 s	ν_4 NH_4^+
				1358 m			
					1200 wbr	1273 wbr	ν_2 D_2O
					1124 wbr		
					1106 w	1110 w	ν_4 ND_4^+
937 vs	937 s	939 s	937 s		937 s		
910 mbr	910 mbr	910 m	911 w	919 s	911 m	910 s	ν_s Mo–O_c
891 w	893 w	896 m	895 m		896 mbr		
				889 s			
867 w				871 vs	867 wbr	870 vsbr	ν_{as} Mo–O_c
					848 wbr		
722 wbr	728 wbr	729 wbr	716 w				ν_r H_2O

TABLE 5—*Continued*

$(NH_4)_6[TeMo_6O_{24}]\cdot Te(OH)_6\cdot 7H_2O$					$(ND_4)_6[TeMo_6O_{24}]\cdot Te(OH)_6\cdot 7D_2O$		
Raman							
c(bb)a A_g	*c(ab)a* A_g	*c(ac)a* B_g	*c(bc)a* B_g	IR	Raman	IR	Assignments
688 w	688 w		684 w		685 vwbr		ν_s Mo–O_b–Mo
				660 sbr		678–630 sbr	ν_{as} Mo–O_b–Mo
				599 s		591 m	
					582 w	582 m	ν_3 TeO_6
560 m	556 w	548 w	562 w	540 m			
510 w	523 w	510 vw	539 w	530 w	538 vw	534 m	δ_s O_c–Mo–O_c
446 wbr	466 w	448 vw	460 vw	483 w		450–	
	430 vw	418 vw	437 w	442 s		390 mbr	ν_4 TeO_6
		399 vw	398 w	392 w	410 wbr		
386 wbr	386 w	387 w	389 vw				δ_{as} O_c–Mo–O_c
358 mbr	352 mbr	352 wbr	357 w			350 wbr	
			351 m	349 mbr			ν_s Mo–O_a–Mo
	324 w		332 vw		318 mbr	311 vw	ν_{as} Mo–O_a–Mo,
	318 w	312 w	320 w	305 m	292 wbr	302 vw	ν_5 TeO_6
276 vw	268 vw		260 w		280 vw	291 w	ν_6 TeO_6
228 mbr	226 mbr	229 mbr	224 m	228 m	226 mbr		δ Mo–O–Mo
188 m	184 w	183 w	189 w		182 vw		
147 m	146 w				150 wbr		External modes
111 m	105 m	111 m	108 m				

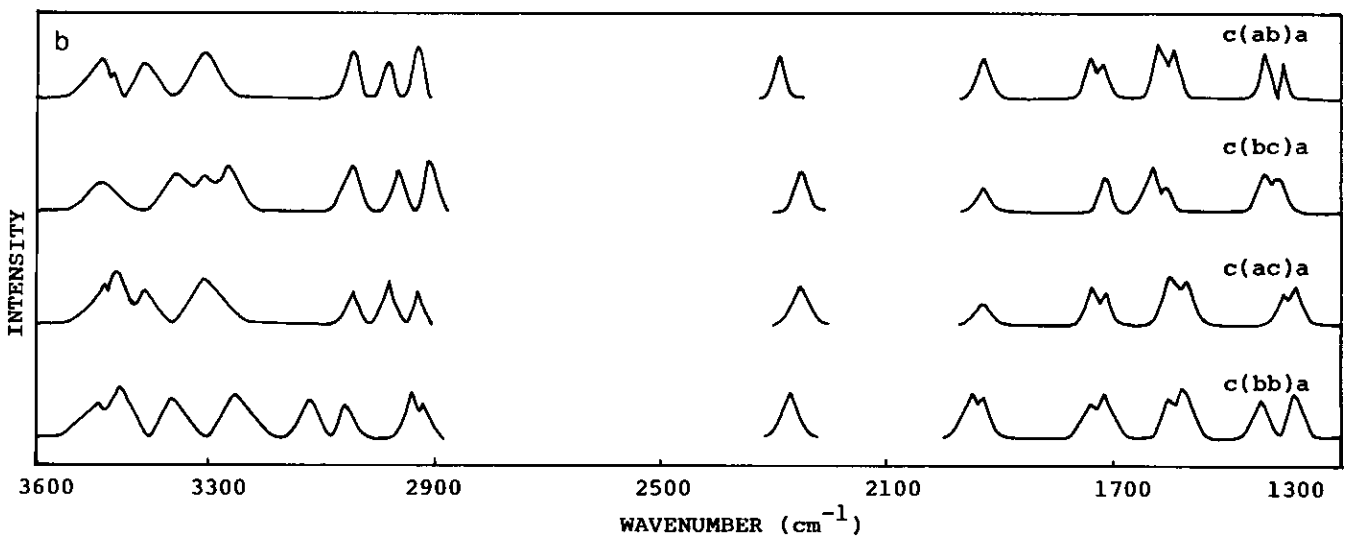

FIG. 6b. Raman spectra of $(NH_4)_6[TeMo_6O_{24}]\cdot Te(OH)_6\cdot 7H_2O$ in the 1300–3600 cm^{-1} region for the *c(bb)a*, *c(ac)a*, *c(bc)a*, and *c(ab)a* orientations.

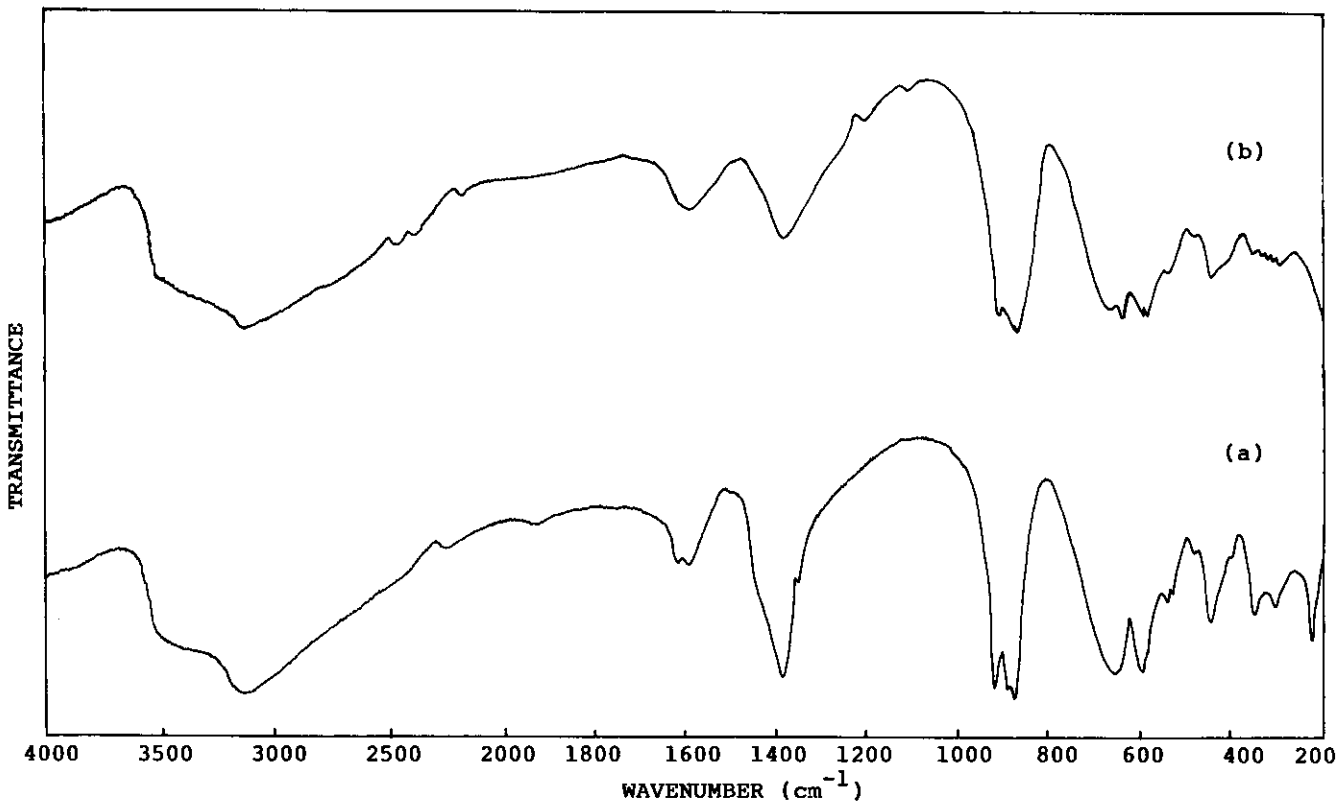

FIG. 7. Infrared spectra of (a) $(NH_4)_6[TeMo_6O_{24}] \cdot Te(OH)_6 \cdot 7H_2O$ and (b) $(ND_4)_6[TeMo_6O_{24}] \cdot Te(OH)_6 \cdot 7D_2O$ in the 200–4000 cm^{-1} region.

NH_4 Vibrations

The nondegenerate symmetric stretching vibrations of NH_4^+ ion give a doublet in all the orientations of NTMH2 crystal. The correlation field effect may be the reason for such a splitting of the ν_1 mode in this crystal. The infrared spectrum in this region gives a strong broad absorption ranging from 2922 to 3320 cm^{-1}. This is assigned to the symmetric and asymmetric stretching vibrations of NH_4^+ ion. However, the triply degenerate asymmetric stretching vibrations retain their degeneracy in the Raman spectra. A complete removal of degeneracy is observed for the doubly degenerate symmetric bending mode and a partial lifting of degeneracy for the triply degenerate asymmetric bending mode in the Raman spectra (Fig. 6b). Similar to that in NTMH1, the appearance of the combination bands of $\nu_2 + \nu_4$ and $\nu_2 + \nu_6$ in the Raman and infrared spectra of NTMH2 crystal shows that the NH_4^+ ions do not rotate freely in this crystal and that they form hydrogen bonds with MoO_6 octahedra. The isotopic shift ratio of 1.29 shows that N–H $\cdots$ O bonds form an asymmetry potential in NTMH2 as in NTMH1 crystal.

H_2O/D_2O Vibrations

In NTMH2 also, the stretching vibrations of water molecules give a number of bands with frequencies considerably shifted from the free state values, indicating the presence of hydrogen bonds of various strengths (Fig. 7). The observed stretching and bending modes of water molecules are assigned and the results are given in Table 5. On deuteration these bands are shifted toward lower wavenumber regions.

CONCLUSIONS

The Te–O vibrations and the bridging and terminal Mo–O vibrations observed in the IR and Raman spectra confirm a finite $[TeMo_6O_{24}]^{6-}$ heteropolyanion in all three crystals. TeO_6 octahedra is considerably distorted in NTMH1 and NTMH2 crystals, while the distortion is less in KTMH crystal. NH_4^+ ion is not rotating freely in the crystalline lattice and the N–H $\cdots$ O bonds form an asymmetric potential in both the ammonium-containing crystals. Stretching and bending vibrations of water molecules show hydrogen bonds of various strengths in all three crystals. Two crystallographically distinct water molecules are identified in KTMH crystal.

REFERENCES

1. P. C. H. Mitchell, Ed., "The Chemistry and Uses of Molybdenum." Climax Molybdenum Co., New York, 1974.

2. O. Nakamura, T. Kodama, I. Ogino, and Y. Miyake, *Chem. Lett.*, 17 (1979).
3. F. J. Keggin, *Proc. R. Soc.* **144,** 75 (1934).
4. H. T. Evans, *Acta Crystallogr. Sect. B* **30,** 2095 (1974).
5. H. T. Evans, *J. Am. Chem. Soc.* **70,** 1291 (1948).
6. H. T. Evans, *J. Am. Chem. Soc.* **90,** 3275 (1968).
7. R. Grabowski, A. Gumula, and J. Sloczynski, *J. Phys. Chem. Solids* **41,** 1027 (1980).
8. W. G. Fateley, F. R. Dollish, N. T. McDevitt, and F. F. Bentley, "Infrared and Raman Selection Rules for Molecular and Lattice Vibrations—The Correlation Method." Wiley, New York, 1972.
9. G. M. Clark and W. P. Doyle, *Spectrochim. Acta* **22,** 141 (1966).
10. M. Liegeois-Duyckaerts and P. Tarte, *Spectrochim. Acta Part A* **30,** 1771 (1974).
11. G. Blasse and A. F. Corsmit, *J. Solid State Chem.* **6,** 513 (1973).
12. C. R. Deltcheff, M. Fourniev, R. Franck, and R. Thouvenot, *Inorg. Chem.* **22,** 207 (1983).
13. B. L. George, G. Aruldhas, and I. L. Botto, *J. Mat. Sci. Lett.* **11,** 1421 (1992).
14. R. Bhattacharjee, *J. Raman Spectrosc.* **21,** 491 (1990).
15. F. D. Hardcastle and I. E. Wachs, *J. Raman Spectrosc.* **21,** 683 (1990).
16. D. S. Kim, K. Segawa, T. Soeya, and I. E. Wachs, *J. Catal.* **136,** 539 (1992).
17. R. Mattes, K. Mennemann, N. Jackel, H. Rieskamp, and H. J. Brockmeyer, *J. Less-Common Met.* **76,** 199 (1980).
18. A. B. Kiss and S. Hally, *Acta Chim. Acad. Sci. Hung.* **75,** 147 (1972); A. B. Kiss, *Acta Chim. Acad. Sci. Hung.* **75,** 351 (1963).
19. F. A. Cotton and R. A. Wing, *Inorg. Chem.* **4,** 867 (1965).
20. R. Allman and W. Haase, *Inorg. Chem.* **15,** 804 (1976).
21. G. Blasse and W. Hordijk, *J. Solid State Chem.* **15,** 395 (1972).
22. D. Philip, S. Abraham, and G. Aruldhas, *J. Raman Spectrosc.* **21,** 521 (1990).
23. R. Haresh, P. Rajagopal, G. Aruldhas, and G. Keresztury, *Spectrochim. Acta Part B* **48,** 1453 (1992).
24. S. N. Vinogradov and R. H. Linnel, "Hydrogen Bonding." Van Nostrand–Reinhold, New York, 1971.
25. A. Novak, "Mathematical and Physical Sciences" (T. M. Theophanides, Ed.), NATO Advanced Study Institute, Series C. Reidel, Dordrecht, 1979.
26. K. Nakamoto, "Infrared Spectra of Inorganic and Coordination Compounds," 2nd ed. Wiley, New York, 1970.
27. E. L. Varetti, E. L. Fernandez, and A. B. Altabef, *Spectrochim. Acta Part A* **47,** 1767 (1991).
28. I. A. Oxton, O. Knop, and M. Falk, *Can. J. Chem.* **54,** 892 (1976).
29. T. C. Wadington, *J. Chem. Soc.* 4340 (1958).
30. J. T. R. Dunsmuir and A. P. Lane, *Spectrochim. Acta Part A* **28,** 45 (1972).
31. A. Novak, *Struct. Bonding* **18,** 177 (1977).